precipitation events cause extreme streamflow in the Godavari, while the rest depends on other factors.

One notable observation made in the present study is that several extreme peak streamflows correspond to strong La *Niña* years. This requires further studies to establish the connection of ENSO events with the sensitivity of peak streamflow not only in the Godavari, but also other Peninsular Indian catchments. While our primary aim was limited to determining the trends in peak streamflow, this study revealed possibly a greater role of mesoscale changes in climatic conditions, topographic response, and anthropogenic factors that may significantly influence the erratic peak streamflow behaviour in the Godavari basin. Moreover, as the high magnitude flooding events in Peninsular India are related to extreme annual streamflows, the increasing trends in the northern stations (Indravati sub-catchment) indicate the alarming potential of increasing flood intensity that may affect larger populations and infrastructures in those regions in the future.

1. Bloschl, G. *et al*., Changing climate both increases and decreases European river floods. *Nature*, 2019, **573**, 108–111.
2. Marsh, T. and Harvey, C. L., The Thames flood series: a lack of trend in flood magnitude and a decline in maximum levels. *Hydrol. Res*., 2012, **43**, 203–214.
3. Lutz, A. F., Immerzeel, W. W., Shrestha, A. B. and Bierkens, M. F. P., Consistent increase in High Asia's runoff due to increasing glacier melt and precipitation. *Nature Climate Change*, 2014, **4**, 587–592.
4. Veh, G., Korup, O., Specht, S. V., Roessner, S. and Walz, A., Unchanged frequency of moraine-dammed glacial lake outburst floods in the Himalaya. *Nature Climate Change*, 2019, **9**, 379–383.
5. Mishra, V. and Shah, H. L., Hydroclimatological perspective of the Kerala flood of 2018. *J. Geol. Soc. India*, 2018, **92**, 645–650.
6. Padma, T. V., Minng and dams exacerbated devastating Kerala floods. *Nature*, 2018, **561**, 13–14.
7. Shugar, D. H. *et al*., A massive rock and ice avalanche caused the 2021 disaster at Chamoli, Indian Himalaya. *Science*, 2021, **373**, 300–306.
8. Sudheer, K. P., Bhallamudi, S. M., Narasimhan, B., Thomas, J., Bindhu, V. M., Vema, V. and Kurian, C., Role of dams on the floods of August 2018 in Periyar river basin, Kerala. *Curr. Sci.*, 2019, **116**, 780–794.
9. Ranger, N. *et al*., An assessment of the potential impact of climate change on flood risk in Mumbai. *Climate Change*, 2011, **104**, 139–167.
10. Biksham, G. and Subramanian, V., Sediment transport of the Godavari River basin and its controlling factors. *J. Hydrol*., 1988, **101**, 275–290.
11. Das, S., Sangode, S. J. and Kandekar, A. M., Recent decline in streamflow and sediment discharge in the Godavari basin, India (1965–2015). *Catena*, 2021, **206**, 105537.
12. Das, S., Dynamics of streamflow and sediment load in Peninsular Indian rivers (1965–2015). *Sci. Total Environ.*, 2021, **799**, 149372.
13. Roxy, M. K. *et al.*, A threefold rise in widespread extreme rain events over central India. *Nature Commun.*, 2017, **8**, 1–11.
14. Garg, S. and Mishra, V., Role of extreme precipitation and initial hydrologic conditions on floods in Godavari river basin, India. *Water Resour. Res*., 2019, **55**, 9191–9210.
15. Mann, H. B., Nonparametric tests against trend. *Econometrica*, 1945, **13**, 245–259.
16. Kendall, M. G., *Rank Correlation Methods*, Griffin, London, UK, 1975.
17. Sen, P. K., Estimates of the regression coefficient based on Kendall's tau. *J. Am. Stat. Assoc.*, 1968, **63**, 1379–1389.
18. Hamed, K. H. and Rao, A. R., A modified Mann–Kendall trend test for autocorrelated data. *J. Hydrol.*, 1998, **204**, 182–196.
19. Das, S. and Gupta, A., Multi-criteria decision based geospatial mapping of flood susceptibility and temporal hydro-geomorphic changes in the Subarnarekha basin, India. *Geosci. Front.*, 2021, **12**, 101206.
20. Das, S. and Scaringi, G., River flooding in a changing climate: rainfall–discharge trends, controlling factors, and susceptibility mapping for the Mahi catchment, Western India. *Nat. Hazards*, 2021, **109**, 2439–2459.
21. Wasko, C. and Sharma, A., Steeper temporal distribution of rain intensity at higher temperatures within Australian storms. *Nature Geosci.*, 2015, **8**, 527–529.
22. Berghuijs, W. R., Harrigan, S., Molnar, P., Slater, L. J. and Kirchner, J. W., The relative importance of different flood-generating mechanisms across Europe. *Water Resour. Res.*, 2019, **55(6)**, 4582–4593.

ACKNOWLEDGEMENTS. S.D. thanks UGC-India for financial support. We thank the Heads, Department of Geography and Department of Geology, Savitribai Phule Pune University, for providing necessary facilities to carry out this study. We also thanks Prof. Rajiv Sinha (Subject Editor) and an anonymous reviewer for their insightful comments and suggestions that helped improve the manuscript.

Received 17 January 2022; accepted 12 March 2022

doi: 10.18520/cs/v122/i9/1085-1089

Numerical analysis of heat dissipation through granite and clay in the multi-barrier system of a geological disposal facility

Binu Kumar[1,*], A. K. Verma[2], R. K. Bajpai[1] and T. N. Singh[3]

[1]Homi Bhabha National Institute, Mumbai 400 094, India
[2]Indian Institute of Technology (BHU), Varanasi 221 005, India
[3]Indian Institute of Technology Bombay, Mumbai 400 076, India

High-level heat-emitting long-lived vitrified radioactive waste produced during recycling of the spent nuclear fuel is under consideration for permanent disposal in deep geological formations with appropriate thermomechanical, hydrogeological and geochemical properties. The capability of these rock formations ensuring long-term confinement and isolation of such waste from the environment is significantly controlled

*For correspondence. (e-mail: binu@barc.gov.in)

by their efficiency in smoothly dissipating the heat emanating from the waste. A number of rock types such as basalt, granite, clay stones, volcanic tuff, argillites, etc. are being evaluated worldwide as well as in India. In this study, a granite from Jalore and bentonite from Barmer, both from Rajasthan, India, have been evaluated for their heat dissipation capacity. The study revealed that the temperature within granite at the centre of the canister reached 55.21°C, resulting in a thermal stress of 25.50 MPa. Bentonite experienced a temperature of 67.42°C in the central part with maximum thermal stress and displacement of 1.78 MPa and 0.446 mm respectively. A displacement of 0.997 mm was recorded at the granite–bentonite interface. Thus, no significant microcrack formation or undesirable displacement was observed within the granite as well as in bentonite, suggesting their capability to isolate and confine the heat-emitting source for extended periods.

Keywords: Bentonite, deep geological repository, granite, radioactive waste, thermo-mechanical analysis.

HEAT-emitting high-level radioactive waste is generated during reprocessing of radioactive spent fuels received from nuclear reactors[1–3]. A deep geological repository (DGR) in suitable geological formations is considered worldwide for permanent disposal of such radioactive waste. These facilities are expected to provide for isolation and confinement of radioactive waste over tens of thousands of years until their radioactive decay reduces to safe natural levels[4].

In India, granitic rocks due to their widespread occurrence, high mechanical strength and low porosity are under active consideration for serving as DGR at depths of 500–700 m. The DGR facility relies on multi-barrier natural and engineered layers (i.e. host rock, swelling clay, canisters and vitrified high-level waste) for long-term protection against release of radioactive waste into the biosphere, even in the distant future. A typical DGR is shown in Figure 1 and a layout of DGRs can accommodate up to 10,000 canisters loaded with waste. Radioactive decay of isotopes present in the waste causes continuous heat flux from these canisters, and hence disposal will result in the build-up of heat plume within the rock mass and clay liner. The temperature induces thermal stress and displacement within the rock mass due to long-term thermo-mechanical interaction between bentonite and the granite rock. This controls the evolution of thermal field within a DGR[5–8]. Most of the DGRs worldwide aim to maintain temperatures below 100°C within any part of the repository at any point in time. Smooth dissipation of heat across bentonite and host rock, say granite, thus is the key requirement for providing safe isolation of radioactive waste. It is a worldwide practice to first analyse a single canister with a multi-barrier system[9,10], followed by multiple canisters[11,12] and finally the full-scale repository[13].

In line with the above approach, a single canister has been analysed in the present study in the first phase. The objective of this study is to estimate the thermo-mechanical stability of a granite from Jalore and bentonite from Barmer, both in Rajasthan, India, which can be used in constructing a DGR facility. The study estimates the thermo-mechanical stability of the rocks for long-term exposure to thermal load due to heat emitting waste canister. Hence, numerical simulation of a metre-scale system over a time period of 340 days to evaluate heat dissipation, resultant thermal stresses, strain and displacement using key thermal and mechanical properties of these rocks and clay is carried out. The simulation is performed in three-dimensional finite element (FE) in-house developed coupled code. Time-dependant variations in vital parameters like temperature, thermal strain, stress and displacement have been estimated and critically examined at key locations in the system.

The Jalore granite belongs to the late Proterozoic Malani igneous suite (750–730 Ma) and occurs extensively in the Jalore district of Rajasthan. The granite sample was obtained from a quarry at Bala (lat. 25°49′N and long. 72°11′E) in the Jalore district. Major minerals in the Jalore granite are quartz, albite, microcline and orthoclase with minor amounts of biotite, chlorite and accessory minerals like hematite, magnetite, titanite and zircon. The major elements composition is 71.22% SiO_2, 15.50% Al_2O_3, 5.36% K_2O, 3.31% Na_2O, 1.39% FeO, 0.71% CaO and 0.25% TiO_2. Bentonite used in this study was sampled from Akli mine, Barmer district, Rajasthan (lat. 26°03′N and long. 71°14′E). The physico-chemical properties of bentonite were estimated following ASTM procedures (ASTM D4318, D7928-17, D720, D698)[14]. X-ray diffraction analysis of bentonite shows montmorillonite, kaolinite, quartz and accessory minerals, including almandine, anatase, goethite, rutile, ilmentite and zircon. Table 1 shows the mechanical and thermal properties of Jalore granite and Barmer bentonite. The obtained properties of clay and granite, i.e. conductivity, specific heat, etc. are in line of earlier studies[14,15].

Three-dimensional FE model geometry for Jalore granite, Barmer bentonite and the heat-emitting waste canister was developed using in-house FE coupled code (Figure 2). The granite and clay were modelled as ten-node brick elements having displacements along the x, y and z axis, and temperature as the degree of freedom at each node. The waste canister was modelled as a rigid one and its input temperature time history was transferred onto the inner surface of bentonite (Figure 3). The FE model was discretized using more than 50,000 three-dimensional brick elements. The granite rock and bentonite layer were modelled as Mohr–Coulomb material. In the model, mechanical (rigid and fixed support) and thermal (temperature time history and convective surface) boundary conditions were applied to the canister and clay interface. The outer wall of the granite block was

Table 1. Mechanical and thermal properties of granitic rock and compacted bentonite

Properties	Granite rock	Compacted bentonite
Shear modulus (GPa)	20.10	0.243
Bulk modulus (GPa)	33.05	0.321
Density (kg/m^3)	2700	1800
Tensile Strength (GPa)	0.0125	–
Cohesion (GPa)	0.060	0.0015
Friction angle	58	48
Geological strength index	70	–
Porosity	0.05	0.3
Thermal conductivity (W/m K)	2.30	1.65
Specific heat (J/kg K)	1510	875
Thermal expansion coefficient (1/K)	2e-6	3.5e-5
UCS (MPa)	110	15

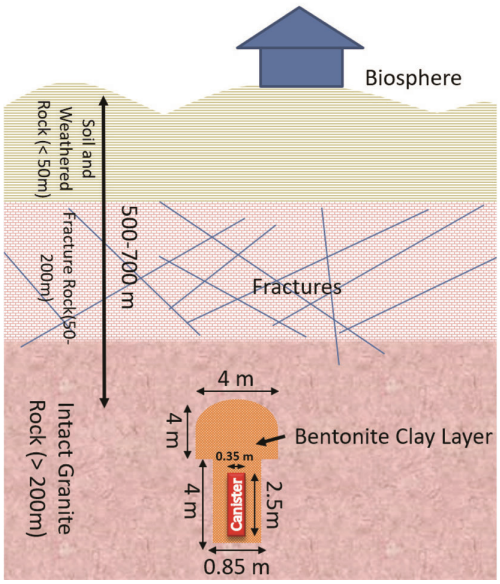

Figure 1. General layout of a typical deep geological repository (not to scale).

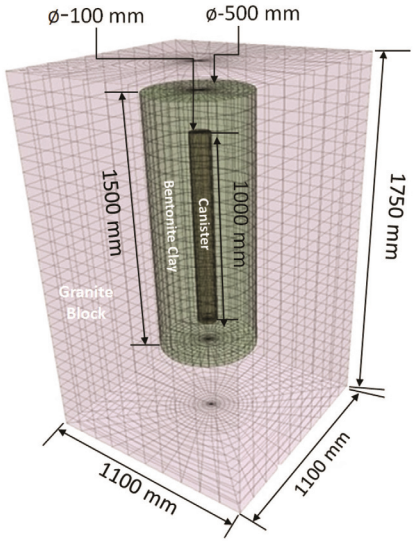

Figure 2. Three-dimensional finite element mesh of the model used in this study.

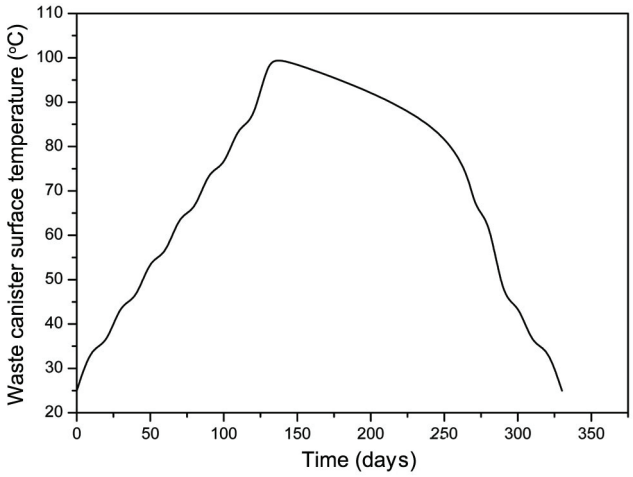

Figure 3. Temperature history profile of the waste canister.

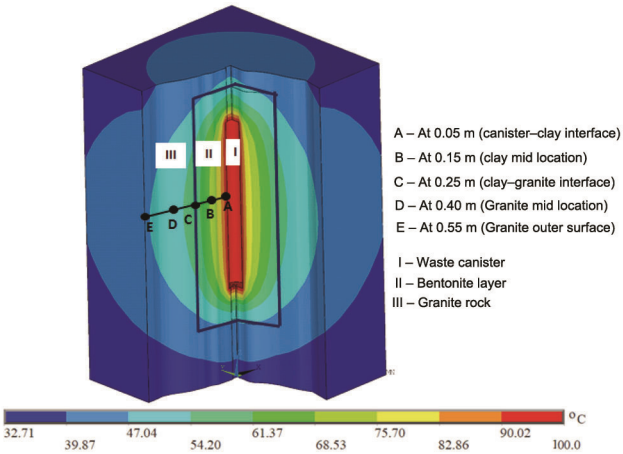

Figure 4. Temperature profile of the model (cut view) at 140 days.

subjected to an atmospheric temperature of 25°C. Steady air surface convective heat dissipation was considered in the analysis.

The time-dependant heat-flux emission pattern from the waste canister embedded in the granite rock was introduced in the model by controlling the heat output of

Table 2. Variation of maximum temperature, thermal strain, stress and displacement

Parameters	Details of location (see Figure 4)				
	A (Canister–clay interface)	B (Clay mid location)	C (Clay–granite interface)	D (Granite mid location)	E (Granite surface)
Temperature (°C)	97.81	67.42	59.09	55.21	50.69
Thermal strain (mm/mm)	0.00030	0.00032	0.000389	0.000274	0.000137
Thermal stress (MPa)	1.78	1.78	35.72	25.50	11.56
Displacement (mm)	0.000	0.446	0.997	0.334	0.000

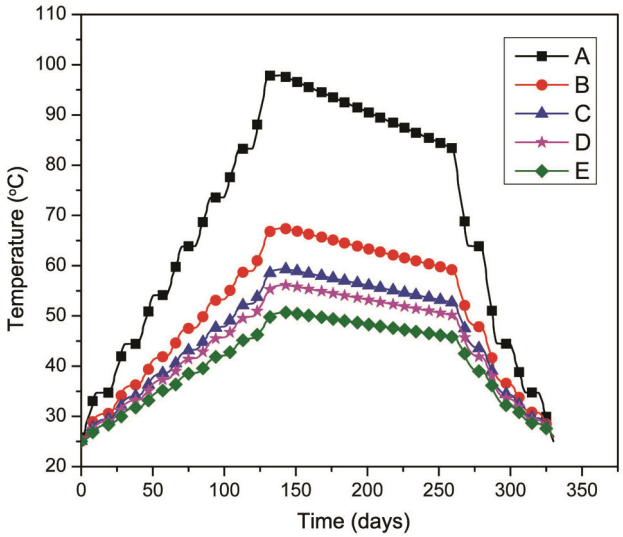

Figure 5. Temperature history at different locations in the mid plane.

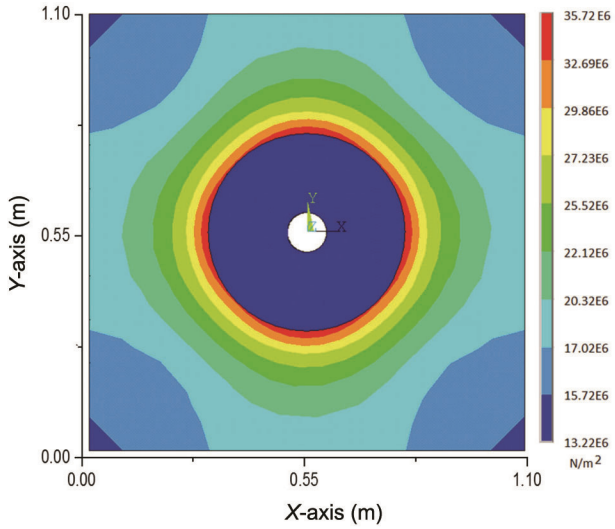

Figure 6. Thermal stress contour (mid plane) at 140 days.

the canister. The waste canister surface temperature gradually increased at a rate of 1°C/10 days from 25°C to 100°C. A temperature of 100°C was attained on the 140th day (Figure 3). Subsequently, it was gradually reduced to attain the initial temperature of 25°C in another 200 days.

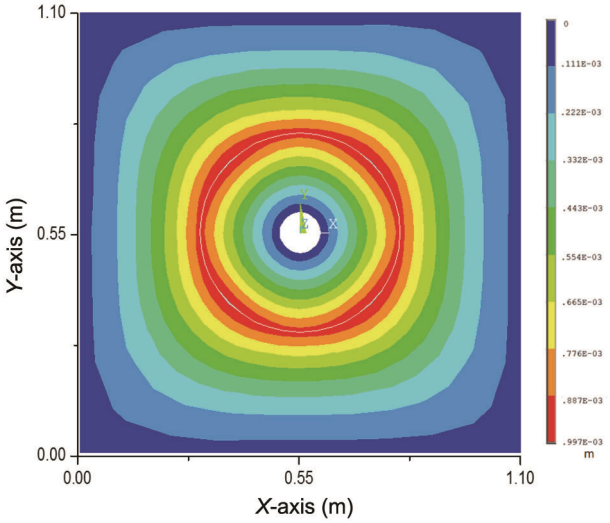

Figure 7. Displacement contour (mid plane) at 140 days.

A total of five-sampling points on the mid plane were fixed in the modelled system to record the time-dependant evolution of temperature, stress, strain and displacement (Figure 4). Table 2 shows the maximum stress, temperature, strain and displacement recorded during the complete time span of the analysis. The contour plot of temperature within the system after 140 days showed no adverse or accelerated advancement of heat front over a distance of 0.50 m due to adequate thermal conductivity of the selected granite and bentonite. The midpoint of the bentonite layer experienced a maximum temperature of 67.42°C (Figure 5). Distribution of the resultant thermal stresses across the system indicated a maximum stress build-up of 35.72 MPa at the bentonite–granite interface, mainly on account of the difference in thermal conductivity of the two materials. Figure 6 shows the stress contour plot. The present study reveals that temperature within the granite reaches 35.42°C, 45.82°C and 55.21°C when the waste canister attains a temperature of 50°C, 75°C and 100°C respectively. The corresponding thermal stress values within the granite for these temperatures are 24.40, 24.83 and 25.50 MPa respectively. The magnitude of displacement induced by thermal stress is higher at the bentonite–granite interface due to the coupling of two materials of different rheologies. However, displacement values across the modelled

region do not exceed 1 mm (Figure 7). The displacement in bentonite and granite is thus within desirable levels. Similarly, no significant deformation was noticed within the system; a maximum strain value concentration of 0.000389 mm/mm was noted at the bentonite–granite interface. The thermal stress/unconfined compressive strength ratios for bentonite, granite at their interfaces were of 0.12 and 0.32 respectively. Therefore, both the materials are by and large stable with the possibility of minor spalling.

The thermo-mechanical numerical modelling using in-house FE coupled code was carried out to estimate thermal mechanical–interaction stability, design and layout of a typical Indian DGR near field system using Jalore granite and barmer bentonite. The results reveal that layers of the selected site-specific granite and bentonite will remain stable under continuous thermal load with the possibility of minor microfracturing at the bentonite–granite interface. The study further shows that granite from Jalore and bentonite from Barmer have adequate strength and thermal conductivity for smooth heat dissipation without undergoing any appreciable degradation. It is, however, emphasized that this study addresses only one of the desirable aspects of the host rock, i.e. heat dissipation. Therefore, we do not recommend the final suitability of these rocks towards hosting heat-emitting waste. Further research on the Jalore granite evaluating hydraulic–geochemical–radiological and mechanical properties must be carried out to assess the granite area for housing a DGR. Similar studies must be taken up on the other granitic massifs in India. Detailed exploration of bentonite and its characterization are also required.

1. Verma, A. K., Gautam, P., Singh, T. N. and Bajpai, R. K., Discrete element modelling of conceptual deep geological repository for high-level nuclear waste disposal. *Arab. J. Geosci.*, 2015, **8**, 8027–8038.
2. Raj, K., Prasad, K. K. and Bansal, N. K., Radioactive waste management practices in India. *Nucl. Eng. Des.*, 2006, **236**(7–8), 914–930.
3. Börgesson, L. and Jan, H., Hydraulic bentonite/rock interaction in FEBEX experiment. In *Advances in Understanding Engineered Clay Barriers*, Proceedings of the International Symposium on Large Scale Field Tests in Granite, 2005, pp. 353–372.
4. Liu, Y. M. *et al.*, Design and validation of the THMC China-mock-up test on buffer material for HLW disposal. *J. Rock Mech. Geotech. Eng.*, 2014, **6**(2), 119–125.
5. Harris, A. F., McDermott, C. I., Bond, A., Thatcher, K. and Norris, S., A non-linear elastic approach to modelling the hydro-mechanical behaviour of the SEALEX experiments on compacted MX-80 bentonite. *Environ. Earth Sci.*, 2016, **75**, 1445.
6. Zhao, H. G., Shao, H., Kunz, H., Su, R. and Liu, Y. M., Numerical analysis of thermal process in the near field around vertical disposal of high-level radioactive waste. *J. Rock Mech. Geotech. Eng.*, 2014, **6**(1), 55–60.
7. Yang, S. Y. and Yeh, H. D., Modelling transient heat transfer in nuclear waste repositories. *J. Hazard. Mater.*, 2009, **169**, 108–112.
8. http://www.iaea.org/inis/collection/NCLCollectionStore/_Public/28/076/28076961 (accessed on 21 April 2021).
9. Ali, S. D. and Kim, J., A numerical simulation of thermo-mechanical behavior of the intact rock in response to the borehole heater test. *Ann. Nucl. Energy*, 2017, **101**, 301–311.
10. Guo, R., Thermohydromechanical modelling of the buffer/container experiment. *Eng. Geol.*, 2011, **122**, 303–315.
11. Dixon, D., Chandler, N., Graham, J. and Gray, M. N., Two large-scale sealing tests conducted at atomic energy of Canada's underground research laboratory: the buffer–container experiment and the isothermal test. *Can. Geotech. J.*, 2002, **39**, 503–518A.
12. Gens, M. S., Guimarães, L., Alonso, E. E., Lloret, A., Olivella, S., Villar, M. V. and Huertas, F., A full scale *in situ* heating test for high level nuclear waste disposal. Observations, analysis and interpretation. *Géotechnique*, 2009, **59**, 377–399.
13. Sonnenthal, E., Ito, A., Spycher, N. and Kawakami, S., Approaches to modelling coupled thermal, hydrological, and chemical processes in the drift scale heater test at Yucca Mountain. *Int. J. Rock Mech. Min. Sci.*, 2005, 698–719.
14. Rao, S. M., Kachroo, T. A., Allam, M. M., Joshi, M. R. and Acharya, A., Geotechnical characterization of some Indian bentonites for their use as buffer material in geological repository. In Proceedings of 12th International Conference of International Association for Computer Methods and Advances in Geomechanics, 2008, pp. 2106–2114.
15. Gautam, P. K., Verma, A. K., Sharma, P. and Singh, T. N., Evolution of thermal damage threshold of Jalore granite. *Rock Mech. Rock Eng.*, 2018, **51**, 2949–2956.

Received 21 July 2021; re-revised accepted 15 March 2022

doi: 10.18520/cs/v122/i9/1089-1093